Chinese Chemical Letters 35 (2024) 109666

Contents lists available at ScienceDirect

Chinese Chemical Letters

journal homepage: www.elsevier.com/locate/cclet

Luminescent terphen[3]arene sulfate-activated FRET assemblies for cell imaging☆

Zhixue Liu, Haiqi Chen, Lijuan Guo, Xinyao Sun, Zhi-Yuan Zhang, Junyi Chen, Ming Dong, Chunju Li*

Tianjin Key Laboratory of Structure and Performance for Functional Molecules, College of Chemistry, Tianjin Normal University, Tianjin 300387, China

ARTICLE INFO

Article history:
Received 30 November 2023
Revised 31 January 2024
Accepted 17 February 2024
Available online 22 February 2024

Keywords:
Luminescent macrocycle
Terphen[3]arene sulfate
Multicharged assembly
Multivalent interactions
Förster resonance energy transfer
Cell imaging

ABSTRACT

Multicharged supramolecular assemblies based on luminescent macrocycle play an important role in extending their optical properties and functions. Herein, we reported macrocyclic supramolecular assemblies based on luminescent terphen[3]arene sulfate (TP[3]AS) and tetraphenylethylene pyridinium (TPE-4Py) through electrostatic interactions, host-guest encapsulation and π-π stacking interactions. Förster resonance energy transfer (FRET) process from TP[3]AS to TPE-4Py was achieved with the energy transfer efficiency of 99.9%, accompanied by TPE-4Py fluorescence emission bathochromic shifted of 15 nm and enhanced by 1.68 times in PBS solution. In contrast, other non-luminescent sulfato-β-cyclodextrin and sulfobutylether-β-cyclodextrin only can enhance the fluorescence intensity of TPE-4Py without bathochromic shift. Due to the strong fluorescence and good stability of TPE-4Py@TP[3]AS, it can be used for optical imaging in living cells, which provided an effective approach for the construction of assembling-confined luminescent biomaterials.

Multicharged supramolecular assemblies based on macrocycles and guest molecules have been wide applied in drug delivery [1,2], luminescent materials [3–5], biomedicine materials [6,7] and other fields. The commonly used macrocycles including crown ether [8–10], cyclodextrins [11–15], cucurbit[*n*]urils [16–20], calix[*n*]arene [21–23], pillar[*n*]arenes [24–30], cyclophanes and cages [31–33], as well as other macrocyclic derivatives [34–36], which can bind guest molecules through the host-guest interactions, electrostatic interactions, hydrophobic interactions, multiple hydrogen bonds, aromatic π-π stacking and ion-dipole interactions, not only can encapsulate the guests for improving their water-solubility and making them more stable in the aqueous solution, but also can assemble guest molecules together for efficiently improving their luminescence properties.

In terms of preferred charged macrocycles, many of them do not have luminescence properties to the best of our knowledge [37–40], which may affect the improvement of the optical properties of the assembly. Generally, the non-luminescent macrocyclic supramolecular assembly was focused on studying the optical behaviors of guest molecules, such as aggregation-induced emission or aggregation-caused quenching [41–43]. However, the assembly based on luminescent macrocyclic hosts usually concentrated on the effect by host-guest interactions, thereby some additional optical phenomena between the hosts and the guests can be realized, such as energy transfer, electron transfer, which could improve their optical properties and endow them with multifunction feature. For example, Stoddart and coworkers reported that tetracationic box can bind porphyrin photosensitizer for the safe delivery into lysosomes and released it at low pH, and the host–guest complex displayed ultrafast photoinduced electron transfer and realized the regulated photodynamic therapy of photosensitizer in cancer cells [44]. Subsequently, they synthesized a tricyclic octacationic cyclophane, XCage, which can encapsulate perylene diimide with high binding affinity, displaying obviously improvement in red-shifted of absorption and emission, turn-on fluorescence and efficient energy transfer [45]. Furthermore, Scherman and coworkers reported that tetracationic cyclophane can bind three dicationic perylene diimides to hexacationic complexes with efficient energy transfer, which have been used as a highly selective melatonin chemical sensor after complexing with cucurbit[7]uril [46]. The above researches proved that luminescent macrocycles can bind guests to generate new optical phenomena and functions, which greatly enriches the performance of the supramolecular assemblies.

Apart from the luminescent cationic cyclophanes and cages, the luminescent extended biphen[*n*]arene derivatives were easy to

☆ This paper is dedicated to the memory of Prof. Jiang Wei.

* Corresponding author.
E-mail address: cjli@shu.edu.cn (C. Li).

https://doi.org/10.1016/j.cclet.2024.109666
1001-8417/

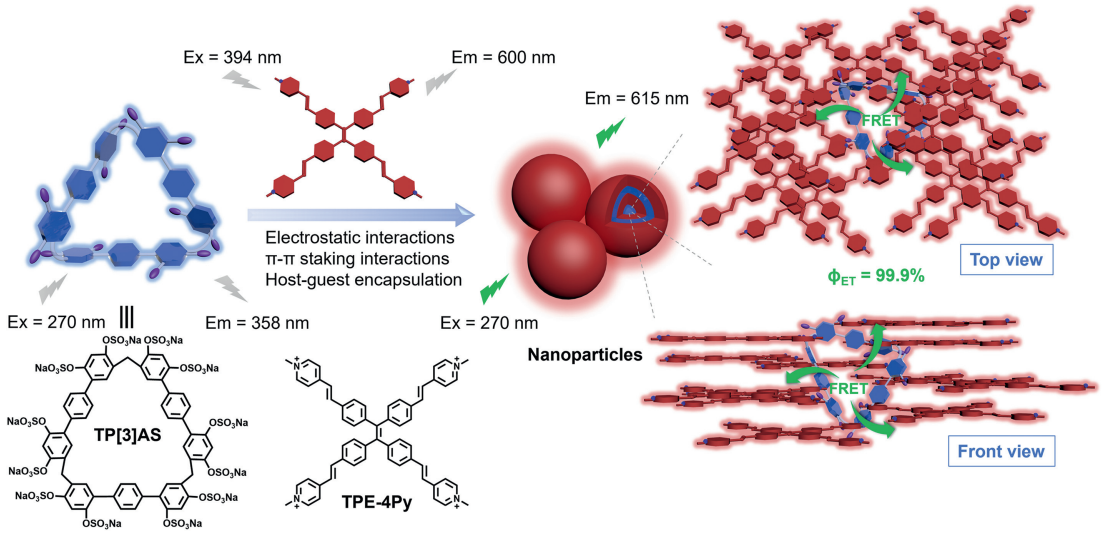

Scheme 1. Schematic illustration of the assembly mechanism between TPE-4Py and TP[3]AS, as well as their FRET process.

synthesize and have been widely used to encapsulate drug and peptide for supramolecular detoxification [47,48], reversal of neuromuscular blockers [49], improve the water-solubility of drugs and other luminescent materials [50,51]. Due to the existence of multiple aromatic units in the structure and the large cavity, the charged extended biphen[*n*]arene derivatives exhibited good luminescence properties, and can encapsulate guests through host-guest interactions, aromatic π-π stacking interactions, as well as the presence of charged groups is conducive to assembly through electrostatic interactions [52,53]. Therefore, multicharged luminescent extended biphen[*n*]arene-based assembly can generate an efficient energy transfer process to the guest molecules, which provide a good platform for the construction and application of luminescent macrocyclic supramolecular assembly.

Herein, we reported terphen[*n*]arene-based supramolecular assemblies by luminescent negatively charged terphen[3]arene sulfates (TP[3]AS) and positively charged tetraphenylethylene pyridinium (TPE-4Py) (Scheme 1). By using the host-guest encapsulation, electrastatic interactions and π-π stacking interactions, the assembly of TPE-4Py@TP[3]AS displayed obvious fluorescence enhancement about 12-fold than TPE-4Py alone in aqueous solution, and the diameter of the resulting nanoparticles of TPE-4Py@TP[3]AS was about 7 nm. Due to the good overlap between the emission of TP[3]AS and absorption of TPE-4Py, the effcient Förster resonance energy transfer (FRET) process was occurred, accompanied by the energy transfer efficiency reached 99.9%. Compared other negatively charged macrocycles, such as sulfato-β-cyclodextrin and sulfobutylether-β-cyclodextrin, the TP[3]AS participated assembly not only displayed fluorescence enhancement, but also endowed the guests with bathochromic shift of 15 nm in PBS buffer solution. With the satisfactory optical properties and good stability of TPE-4Py@TP[3]AS, it can be used for optical imaging inside living cells.

To investigate the assembly behaviors of positively charged TPE-4Py and negatively charged TP[3]AS, their UV–vis absorption and fluorescence changes were first evaluated both in the aqueous and PBS buffer solutions. Upon addition of TP[3]AS, the UV–vis absorption peak of TPE-4Py gradually decreased with the increase of 500 nm absorption in aqueous solution with a bathochromic shift of 3 nm (Fig. 1a), and the fluorescence emission intensity was increased by about 12 times (Fig. 1b). By contrast, after adding TP[3]AS to the PBS solution of TPE-4Py, the UV–vis absorption peak of TPE-4Py not only gradually decreased with the enhance

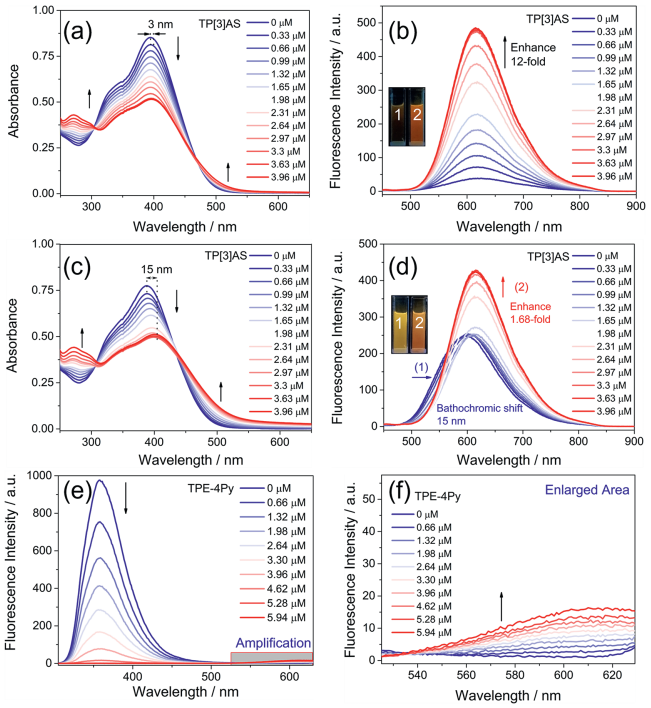

Fig. 1. UV–vis absorption and fluorescence spectra of TPE-4Py (30 μmol/L) upon addition of TP[3]AS (0–3.96 μmol/L) in aqueous solution (a, b) and in PBS solution (c, d) (E_x = 395 nm; slits: 5/10 nm). Inset (b, d): Photographs of (1) TPE-4Py and (2) TPE-4Py@TP[3]AS in aqueous and PBS solution under 365 nm irradiation. (e) Fluorescence spectra of TP[3]AS (1.33 μmol/L) upon addition of TPE-4Py (0–5.94 μmol/L) in aqueous solution (E_x = 270 nm; slits: 5/2.5 nm). (f) Enlarged area in Fig. 1e. μM = μmol/L.

of 500 nm absorption, but also bathochromic shifted by 15 nm (Fig. 1c). Meanwhile, the fluorescence emission spectrum was first bathochromic shifted by about 15 nm during the titration process, and then the intensity was enhanced by about 1.68 times (Fig. 1d). The enhancement of the absorption at 500 nm indicates that TPE-4Py and TP[3]AS were obviously assembled, thus, when excited at 500 nm, a significant fluorescence enhancement of TPE-4Py@TP[3]AS was achieved compared to the TPE-4Py alone (Fig. S1 in Supporting information). The obvious bathochromic shift

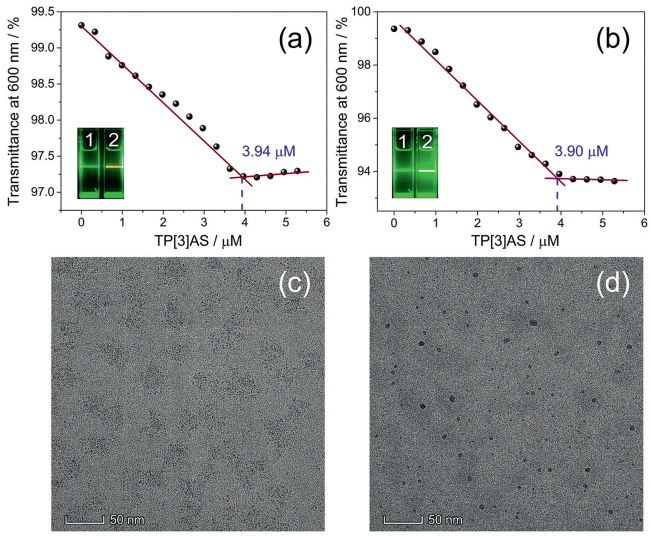

Fig. 2. Optical transmittance changes of TPE-4Py (20 μmol/L) upon addtion of different concentrations of TP[3]AS (a) in aqueous solution and (b) in PBS solution. Inset (a, b): Tyndall effects exhibited by (1) TPE-4Py and (2) TPE-4Py@TP[3]AS. μM = μmol/L. (c, d) TEM image of TPE-4Py and TPE-4Py@TP[3]AS, respectively.

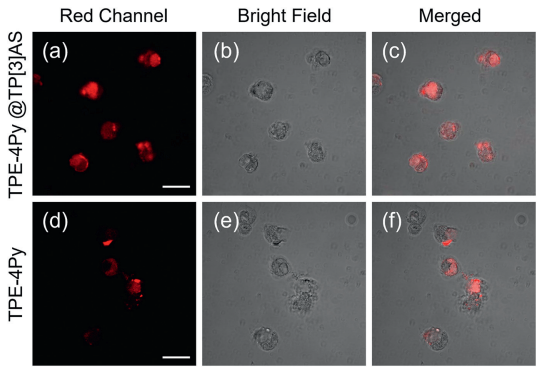

Fig. 3. Confocal fluorescence images of living HeLa cells incubated with TPE-4Py and TPE-4Py@TP[3]AS (scale bar = 20 μm). (a, d) Red channel (E_x = 405 nm, E_m = 550 – 700 nm). (b, e) Bright field. (c, f) Merged images of red channel and bright field.

of UV–vis absorption and fluorescence spectra in the PBS solution may be caused by the host-guest encapsulation, electrostatic interactions, and π-π stacking interactions, which restricted the rotation of TPE-4Py and assembled them together, resulting in greatly enhanced fluorescence intensity and emission spectrum bathochromic shift.

As can be seen from Figs. 1a and c, the absorption peak at 270 nm was increased, which was caused by the increased TP[3]AS concentration. Structually, TP[3]AS possessed blue fluorescence with a maximum emission wavelength of 358 nm, displaying a good overlap with the absorption of TPE-4Py (Fig. S2 in Supporting information). This overlap may generate a FRET process from TP[3]AS (donor) to TPE-4Py (accepetor). Therefore, after gradually adding the TPE-4Py into the TP[3]AS solution, the fluorescence intensity of TP[3]AS decreased significantly to disappear with the enhancement of TPE-4Py intensity (Figs. 1e and f), confirming the existence of energy transfer from the TP[3]AS to TPE-4Py. The energy transfer efficiency was calculated as 99.9% when the donor/acceptor molar ratio is 0.22:1 (Fig. S3 in Supporting information). Compared with the same concentration of TPE-4Py alone, the fluorescence intensity of TPE-4Py@TP[3]AS was enhanced by about 14-times at the same excitation wavelength (Fig. S4 in Supporting information). In addition, the fluorescence spectra of TPE-4Py@TP[3]AS at excitation wavelength of TP[3]AS donor and TPE-4Py acceptor were evaluated in the same system. Both of them displayed similar fluorescence intensity (Fig. S5 in Supporting information), indicating that the weak fluorescence intensity of the TPE-4Py in the assembly is mainly due to the weak fluorescence characteristics of the TPE-4Py itself. Therefore, from the perspective of fluorescence reduction of TP[3]AS and fluorescence enhancement of TPE-4Py, as well as the good overlap between the emission of TP[3]AS and the absorption of TPE-4Py, it can be infered that an effective FRET process was occured from TP[3]AS to TPE-4Py.

On the other hand, the optical transmittance of TPE-4Py and TP[3]AS at 600 nm was measured to further understand their assembly process. As the TP[3]AS content increased, the optical transmittance of TPE-4Py was decreased to a minimum and remain stable when the concentration is greater than 3.94 μmol/L and 3.90 μmol/L in aqueous and PBS solutions, respectively (Figs. 2a and b, Fig. S6 in Supporting information), indicating that TP[3]AS was assembled with TPE-4Py, and the assembly formed by noncovalent interactions is very stable. Based on the concentration ratio of TPE-4Py to TP[3]AS, the optimal molar ratio of TPE-4Py:TP[3]AS is calculated to be about 5.08:1 and 5.13:1 in aqueous and PBS solutions, respectively. Compared with TPE-4Py solution, TPE-4Py@TP[3]AS solution showed a significant Tyndall effect (Figs. 3a and b inset), indicating the formation of abundant supramolecular aggregates. Interestingly, the Tyndall effect of TPE-4Py@TP[3]AS displayed clear orange fluorescence after excitation with a green laser (495 nm), further confirming the efficiency assembly between TPE-4Py and TP[3]AS. Therefore, it can be inferred that TPE-4Py has weak self-aggregation ability, and the addition of TP[3]AS can effectively increase the TPE-4Py aggregation and achieve a stable assembly both in aqueous and PBS solutions.

Subsequently, the morphology of TPE-4Py, TPE-4Py@TP[3]AS was measured by transmission electron microscopy (TEM). The TEM photographs displayed that the TPE-4Py was a nanoparticle with a diameter about 1 nm (Fig. 2c). After assembly with TP[3]AS, the TPE-4Py@TP[3]AS exhibited large nanoparticles with the diameter about 7 nm (Fig. 2d). By increasing the diameter of the nanoparticle, it can be seen that the TPE-4Py and TP[3]AS have assembled together. Meanwhile, the fluorescence quantum yields of TPE-4Py and TPE-4Py@TP[3]AS are measured as 0.76% and 2.46%, respectively (Fig. S7 in Supporting information). The lifetimes of TPE-4Py, TP[3]AS and TPE-4Py@TP[3]AS are calculated as 0.77, 2.97 and 2.73 ns, respectively (Fig. S8 in Supporting information). Through the enhancement of fluorescence quantum yield and lifetime, it can be seen that the assembly of TP[3]AS and TPE-4Py achieved a significant improvement in optical properties.

In order to further confirm the assembly mechanism, we evaluated the ^{1}H NMR of the TPE-4Py, TP[3]AS and TPE-4Py@TP[3]AS. As shown in Fig. S9 (Supporting information), the H_e and H_g of the TPE-4Py in TPE-4Py@TP[3]AS displayed obvious upfield shifts. Meanwhile, due to the deshielding effect of the guest, the H_1, H_3 and H_4 of the host TP[3]AS in TPE-4Py@TP[3]AS exhibited downfield shifts. The passivated part in TPE-4Py@TP[3]AS may come from the assembly between TPE-4Py and TP[3]AS through the electrostatic interactions and π-π stack interactions. The above results confirmed that the TP[3]AS can encapsulate TPE-4Py in its cavity, and the assembly driving forces are mainly from the host-guest encapsulation, electrostatic interactions and π-π stack interactions.

Compare with the non-luminescent macrocyclic assembly, negatively charged sulfato-β-cyclodextrin (SCD) and sulfobutylether-β-cyclodextrin (SBE-βCD) were selected for assembly with TPE-4Py. In aqueous solution, both SCD and SBE-βCD can induce the reduction of UV–vis absorption of TPE-4Py (Fig. S10a in Supporting information), accompanied by the obvious fluorescence enhancement with a hypsochromic shift of about 17 nm (Fig. S10c in Sup-

porting information). Similarly, the assembly of SCD with TPE-4Py in PBS solution also gave the same trend, but the fluorescence intensity was enhanced without any bathochromic shift (Figs. S10b and d in Supporting information). On the other hand, the SBE-βCD can induce the UV–vis absorption bathochromic shift of TPE-4Py in PBS solution, but the fluorescence intensity was decreased with a bathochromic shift of about 8 nm. The results indicated that both SCD and SBE-βCD can enhance fluorescence intensity, but cannot simultaneously enhance fluorescence and induce emission bathochromic shift. As a contrast, TP[3]AS not only increase the fluorescence intensity both in aqueous and PBS solutions, but also resulting in the bathochromic shift of fluorescence emission in PBS solution. Due to the presence of multiple aromatic groups in luminescent TP[3]AS, the intermolecular interactions with TPE-4Py including π-π stacking interactions and host-guest encapsulation can be achieved, leading to the efficient FRET process and emission bathochromic shift. Furthermore, the negatively charged groups was facilitated to assembly with TPE-4Py through the electrastatic interactions, which can restrict the rotation of TPE-4Py and resulting in greatly enhancement of fluorescence intensity.

With the satisfactory optical properties and good stability of TPE-4Py@TP[3]AS in mind, it can be used for fluorescence imaging of complex organisms. The fluorescence imaging was carried out in living HeLa cells. The cells were incubated with TPE-4Py and TPE-4Py@TP[3]AS for 6 h to observe the internalization of the cells. As shown in Figs. 3a-c, the TPE-4Py@TP[3]AS displayed bright fluorescence in the red channel, confirming that TPE-4Py@TP[3]AS could be taken up by cells and give red fluorescence signal. In contrast, the fluorescence observed when incubated with TPE-4Py was relatively weak (Figs. 3d-f). The result indicated that TPE-4Py@TP[3]AS exhibited superior optical imaging capability in living cells.

In summary, we constructed multicharged supramolecular assemblies based on luminescent TP[3]AS and TPE-4Py through host-guest encapsulation, π-π stacking interactions, and electrostatic interactions. TP[3]AS can be served as an excellent donor to transfer energy to TPE-4Py with an energy-transfer efficiency of 99.9%, displaying clear signal amplification of TPE-4Py with a fluorescence emission bathochromic shift about 15 nm in PBS solution, and the formed nanoparticle size of TPE-4Py@TP[3]AS was about 7 nm. In contrast, other non-luminescent negatively charged macrocycles, such as sulfato-β-cyclodextrin and sulfobutylether-β-cyclodextrin, cannot simultaneously enhance fluorescence intensity and emission bathochromic shift. Benefiting from the strong fluorescence and good stability of TPE-4Py@TP[3]AS, cell imaging has been successfully implemented, providing an efficient approach for the construction of assembling-confined luminescent biomaterials.

Declaration of competing interest

The authors declare that they have no known competing financial interests or personal relationships that could have appeared to influence the work reported in this paper.

Acknowledgments

We gratefully acknowledge financial support received from the following: the National Natural Science Foundation of China (Nos. 21971192, 21807038), the Tianjin Municipal Education Commission (No. 2021KJ188), and the China Postdoctoral Science Foundation (No. 2021T140343).

Supplementary materials

Supplementary material associated with this article can be found, in the online version, at doi:10.1016/j.cclet.2024.109666.

References

[1] J. Zhou, G. Yu, F. Huang, Chem. Soc. Rev. 46 (2017) 7021–7053.
[2] X. Ma, Y. Zhao, Chem. Rev. 115 (2015) 7794–7839.
[3] X. Ma, J. Wang, H. Tian, Acc. Chem. Res. 52 (2019) 738–748.
[4] X.K. Ma, Y. Liu, Acc. Chem. Res. 54 (2021) 3403–3414.
[5] Z. Wu, H. Qian, X. Li, T. Xiao, L. Chin, Chem. Lett 35 (2024) 108829.
[6] Z. Liu, W. Lin, Y. Liu, Acc. Chem. Res. 55 (2022) 3417–3429.
[7] Y.C. Pan, X.Y. Hu, D.S. Guo, Angew. Chem. Int. Ed. 60 (2021) 2768–2794.
[8] X. Dong, C. Zhang, X. Dai, et al., Chem. Eur. J. 28 (2022) e202200005.
[9] Y.M. Zhang, X.J. Zhang, X. Xu, et al., J. Phys. Chem. B 120 (2016) 3932–3940.
[10] F. Zhao, Y. Liu, H. Dong, et al., Angew. Chem. Int. Ed. 59 (2020) 10426–10430.
[11] Z. Liu, Y. Liu, Chem. Soc. Rev. 51 (2022) 4786–4827.
[12] Z. Liu, M. Tian, H. Zhang, Y. Liu, Chem. Commun. 59 (2023) 896–899.
[13] Y. Sugita, D. Aoki, M. Tokita, H. Otsuka, Chem. Commun. 58 (2022) 3067–3070.
[14] T. Gu, J. Huang, Y. Yan, Chem. Commun. 59 (2023) 14759–14775.
[15] Y. Sun, L. Jiang, Y. Chen, Y. Liu, Chin. Chem. Lett. 35 (2024) 108644.
[16] G. Wu, F. Li, B. Tang, X. Zhang, J. Am. Chem. Soc. 144 (2022) 14962–14975.
[17] H. Nie, Z. Wei, X.L. Ni, Y. Liu, Chem. Rev. 122 (2022) 9032–9077.
[18] Z. Wang, C. Sun, K. Yang, X. Chen, R. Wang, Angew. Chem. Int. Ed. 61 (2022) e202206763.
[19] M.D. Tian, Z. Wang, X. Yuan, et al., Adv. Funct. Mater. 33 (2023) 2300779.
[20] H.J. Wang, W.W. Xing, Z.H. Yu, et al., Chin. Chem. Lett. (2023) 109183.
[21] S. Li, R. Ma, X.Y. Hu, et al., Adv. Mater. 34 (2022) e2203765.
[22] S.Y. Yao, Y.X. Yue, A.K. Ying, et al., Angew. Chem. Int. Ed. 62 (2023) e202213578.
[23] P. Li, Y. Chen, Y. Liu, Chin. Chem. Lett. 30 (2019) 1190–1197.
[24] B. Shi, K. Jie, Y. Zhou, et al., J. Am. Chem. Soc. 138 (2016) 80–83.
[25] J.R. Wu, G. Wu, Y.W. Yang, Acc. Chem. Res. 55 (2022) 3191–3204.
[26] Y.Y. Chen, X.M. Jiang, G.F. Gong, et al., Chem. Commun. 57 (2021) 284–301.
[27] Y. Mei, Q.W. Zhang, Q. Gu, et al., J. Am. Chem. Soc. 144 (2022) 2351–2359.
[28] Y. Chai, L. Chen, Y. Zhang, et al., Chin. Chem. Lett. 33 (2022) 3003–3006.
[29] C. Peng, W. Liang, J. Ji, et al., Chin. Chem. Lett. 32 (2021) 345–348.
[30] K. Wang, X. Tian, J.H. Jordan, et al., Chin. Chem. Lett. 33 (2022) 89–96.
[31] A. Garci, A.H.G. David, L.Le Bras, et al., J. Am. Chem. Soc. 144 (2022) 23551–23559.
[32] W. Liu, C. Lin, J.A. Weber, et al., J. Am. Chem. Soc. 142 (2020) 8938–8945.
[33] W. Liu, C.L. Stern, J.F. Stoddart, J. Am. Chem. Soc. 142 (2020) 10273–10278.
[34] L.P. Yang, X. Wang, H. Yao, W. Jiang, Acc. Chem. Res. 53 (2020) 198–208.
[35] G.B. Huang, W.E. Li, et al., Chin. Chem. Lett. 29 (2018) 91–94.
[36] Q. Zhang, H. Qian, T. Xiao, R.B.P. Elmes, L. Wang, Chin. Chem. Lett. 34 (2023) 108365.
[37] Z. Li, Y.W. Yang, Acc. Mater. Res. 2 (2021) 292–305.
[38] W.C. Geng, J.L. Sessler, D.S. Guo, Chem. Soc. Rev. 49 (2020) 2303–2315.
[39] J.X. Liu, K. Chen, C. Redshaw, Chem. Soc. Rev. 52 (2023) 1428–1455.
[40] M. Votava, B.J. Ravoo, Chem. Soc. Rev. 50 (2021) 10009–10024.
[41] J. Li, J. Wang, H. Li, et al., Chem. Soc. Rev. 49 (2020) 1144–1172.
[42] T. Xiao, X. Li, L. Zhang, et al., Chin. Chem. Lett. 35 (2024) 108618.
[43] T. Xiao, D. Ren, L. Tang, et al., J. Mater. Chem. A 11 (2023) 18419–18425.
[44] I. Roy, S. Bobbala, R.M. Young, et al., J. Am. Chem. Soc. 141 (2019) 12296–12304.
[45] W. Liu, S. Bobbala, C.L. Stern, et al., J. Am. Chem. Soc. 142 (2020) 3165–3173.
[46] S.T. Ryan, J. Del Barrio, I. Ghosh, et al., J. Am. Chem. Soc. 136 (2014) 9053–9060.
[47] J. Chen, Q. Meng, Y. Zhang, et al., Angew. Chem. Int. Ed. 60 (2021) 11288–11293.
[48] L. Zhao, J. Chen, L. Tian, et al., Adv. Healthcare Mater. 11 (2022) e2200270.
[49] Y. Zhao, L. Chen, J. Chen, et al., Chem. Commun. 59 (2023) 5858–5861.
[50] S. Li, Z.Y. Zhang, J.F. Lv, et al., J. Mater. Chem. A 11 (2023) 4957–4962.
[51] M. Dong, W. Qi, G. Sun, et al., Org. Biomol. Chem. 21 (2023) 6926–6931.
[52] Z.Y. Zhang, C. Li, Acc. Chem. Res. 55 (2022) 916–929.
[53] K. Xu, Z.Y. Zhang, Z. Zhou, C. Li, Chin. Chem. Lett. 33 (2022) 2451–2454.